

RAPID COMMUNICATION

# Cranial Neural Crest Contributes to the Bony Skull Vault in Adult *Xenopus laevis*: Insights From Cell Labeling Studies

JOSHUA B. GROSS\* AND JAMES HANKEN

*Museum of Comparative Zoology, Harvard University, Cambridge, Massachusetts*

**ABSTRACT** As a step toward resolving the developmental origin of the ossified skull in adult anurans, we performed a series of cell labeling and grafting studies of the cranial neural crest (CNC) in the clawed frog, *Xenopus laevis*. We employ an indelible, fixative-stable fluorescent dextran as a cell marker to follow migration of the three embryonic streams of cranial neural crest and to directly assess their contributions to the bony skull vault, which forms weeks after hatching. The three streams maintain distinct boundaries in the developing embryo. Their cells proliferate widely through subsequent larval (tadpole) development, albeit in regionally distinct portions of the head. At metamorphosis, each stream contributes to the large frontoparietal bone, which is the primary constituent of the skull vault in adult anurans. The streams give rise to regionally distinct portions of the bone, thereby preserving their earlier relative position anteroposteriorly within the embryonic neural ridge. These data, when combined with comparable experimental observations from other model species, provide insights into the ancestral pattern of cranial development in tetrapod vertebrates as well as the origin of differences reported between birds and mammals. *J. Exp. Zool. (Mol. Dev. Evol.)* 304B:169–176, 2005. © 2005 Wiley-Liss, Inc.

## INTRODUCTION

The broad developmental capacity of embryonic cranial neural crest (CNC) cells has long interested amphibian developmental biologists (Landacre, '21; Stone, '26; de Beer, '37, '47; Hörstadius, '50; Chibon, '67). Previous studies have successfully resolved many of the varied contributions of CNC to differentiated tissues within embryos and larvae of both frogs and salamanders. Yet, direct evidence of a CNC contribution to many adult-specific features, and especially to the bony adult skull, has remained elusive (Gross and Hanken, 2004). This is especially the case for anurans, in which osteogenesis is an entirely postembryonic event that commences only at the onset of metamorphosis (Trueb, '85). Difficulty in mapping contributions to adult features may be attributed largely to technical problems associated with labeling embryonic neural crest cells in such a way that they and their progeny may be followed over the protracted larval period, which spans the developmental interval between hatching and metamorphosis. Furthermore, at present there are no reliable early markers for osteogenic precursor cells that would allow their unique identification and labeling in early, pre-metamorphic

tadpoles. Consequently, more than 50 years after initial claims of a prominent role of the neural crest in bony skull formation in amphibians (Raven, '31; Andres, '46; Sellman, '46; de Beer, '47; Wagner, '49), we still lack direct evidence of such a relationship.

Detailed fate maps that depict CNC contributions to the bony skull roof, or "skull vault," in vertebrates have been derived for two "model" species: the domestic chicken (Le Lièvre, '78; Noden, '78; Couly et al., '93; Le Douarin and Kalcheim, '99) and the mouse (Morriss-Kay, 2001; Jiang et al., 2002). These reports have revealed important differences in the patterns of embryonic derivation between these species. Comparable data from amphibians would likely inform our understanding of the basal (primitive) pattern of cranial development in tetrapods as well as the evolution of the presumably derived pattern(s)

\*Correspondence to: Joshua B. Gross, Museum of Comparative Zoology, 26 Oxford Street, Cambridge, MA 02138.  
E-mail: jgross@fas.harvard.edu

Grant sponsor: National Science Foundation; Grant number: EF-0334846 (AmphibiaTree); Grant sponsor: The Milton Fund, Harvard University; Grant sponsor: Sigma Xi Grant-in-Aid-of-Research

Received 23 September 2004; Accepted 21 October 2004  
Published online 23 December 2005 in Wiley InterScience (www.interscience.wiley.com). DOI: 10.1002/jez.b.21028

seen in amniotes. Here we report initial results from detailed cell labeling and grafting studies in the clawed frog, *Xenopus laevis*, which are designed to assess the contribution of CNC to the bony skull roof, which forms at metamorphosis. We label neural crest cells with an indelible, fixative-stable fluorescent dextran, which offers an effective and reliable cell marker that is suitable for use over long developmental periods. Our results document a prominent contribution of CNC from all three cranial migratory streams to the frontoparietal bone, the primary constituent of the skull vault in adult anurans.

## METHODS AND MATERIALS

### *Developmental staging and animal care*

Fertilized eggs were obtained and staged according to standard protocols (Sive et al., 2000). Methods for grafting, rearing, and histological

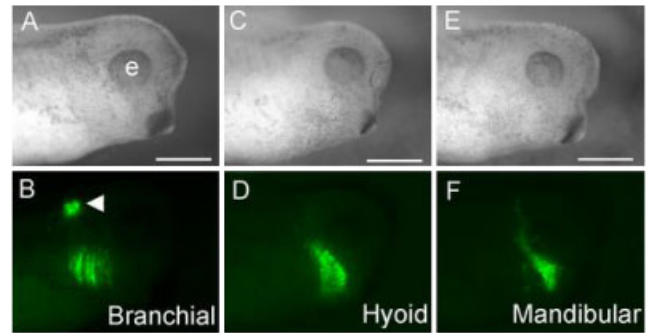


Fig. 1. Bright-field (A, C, E) and fluorescence images of chimeric embryos, NF stage 33/34, following neural crest grafts. Labeled donor embryos were produced by injecting fertilized eggs with fluorescein dextran (Gross and Hanken, 2004). At stage 14, labeled portions of the neural crest corresponding to the three cranial migratory streams were grafted to unlabeled hosts (A, B—branchial; C, D—hyoid; E, F—mandibular). Brightly labeled neural crest cells are migrating ventrally in B, D, and F. Occasionally, portions of the original graft are observed in the neural tube (arrowhead, B). Notes: e, eye; scale bar, 200  $\mu$ m. Lateral views; anterior is to the right.

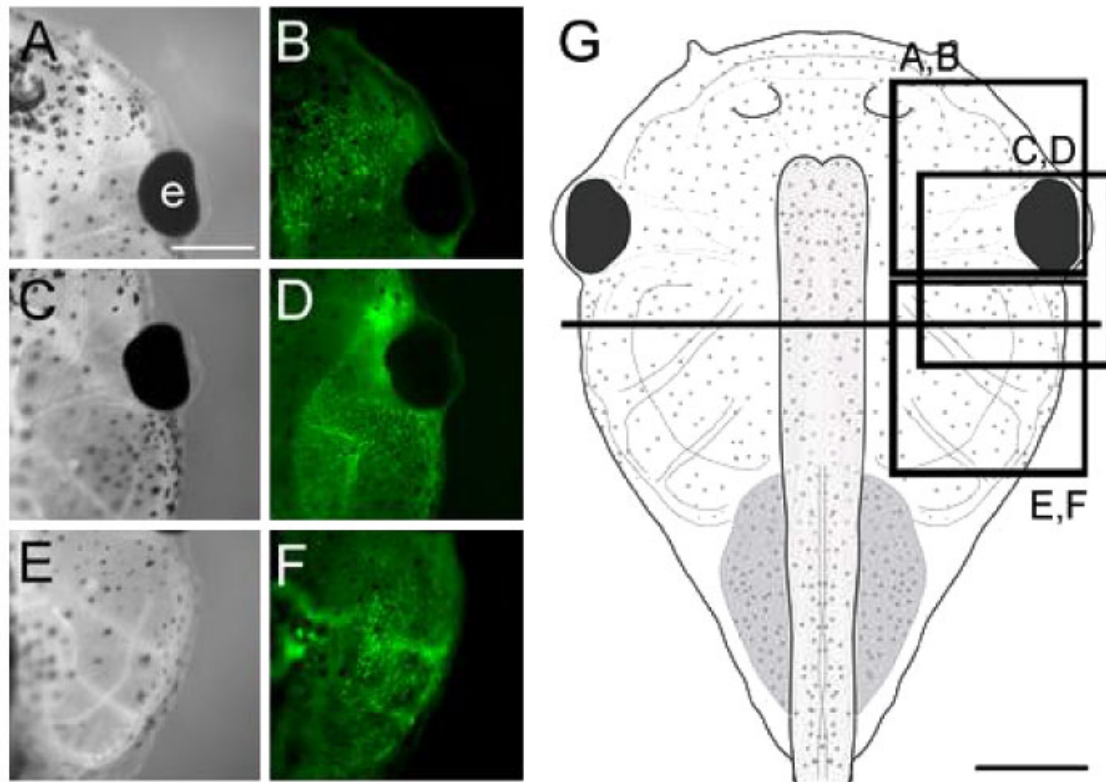


Fig. 2. Ectomesenchymal derivatives of each cranial neural crest (CNC) stream populate regionally distinct portions of the developing head. Six photographs depict portions of the right (grafted) side of the heads of three different chimeric tadpoles. Each chimera received a graft of one of the three migratory streams: mandibular (A, B), hyoid (C, D), or branchial (E, F) at NF stage 41 (A, C, E—bright-field illumination; B, D, F—fluorescence illumination). The schematic tadpole at the right (G) delineates the perspectives shown in the photographs (A–F). Labeled cellular derivatives of each CNC stream (bright punctate areas in B, D, and F) remain at the same anteroposterior level as the corresponding graft; i.e., mandibular stream explants populate anterior regions (A, B) and branchial stream explants (E, F) populate posterior regions, whereas hyoid stream explants populate intermediate regions (C, D). The line depicted in G corresponds with the level of cross section depicted in Fig. 3. Notes: e, eye; scale bar, 100  $\mu$ m.

processing are as reported previously (Gross and Hanken, 2004). Embryonic and larval staging was based on standard normal tables for *X. laevis* (Nieuwkoop et al., '94). Animal care procedures are approved by the Harvard University/Faculty of Arts and Sciences Standing Committee on the use of Animals in Research and Teaching. An Animal Welfare Assurance statement is on file with the university's Office for Laboratory Welfare (OLAW). All experimental animals were sacrificed by immersion in the anesthetic MS-222 (Sigma, St. Louis, MO; catalog number A-5040).

### Fluorescein dextran injections

Fertilized, single-celled embryos were transferred to  $0.3 \times$  MMR (Marc's modified Ringers) solution supplemented with 4% Ficoll (EM Science, Darmstadt, Germany) and stabilized in a Petri dish. Injection needles (1.1 mm outer diameter) were prepared (WPI PUL-1 Micropipette Puller; World Precision Instruments, Sarasota, FL) and bevel-cut to a diameter of 10  $\mu$ m. By using a PicoSpritzer II injection apparatus (Parker Instrumentation, Fairfield, NJ) connected to a vacuum pressure pump, 1  $\mu$ l of fluorescein-labeled dextran (25 mg/ml, 10,000 molecular weight,

lysine-fixable; Molecular Probes, Eugene, OR) was transferred into the needle. Embryos were injected with 5–10 nl of fluorescein dextran and allowed to develop at room temperature (ca. 22–

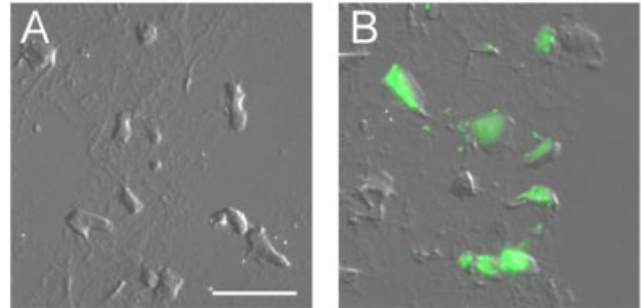


Fig. 3. Undifferentiated mesenchymal cells within the dorsal portion of the larval head are derived in large part from CNC. (A, B) High-magnification (originally  $40 \times$ ) Nomarski images of cross-sections through the dorsal head of a chimeric tadpole (stage 41) lateral to the brain and ventral to the overlying epidermis. (B) Anti-fluorescein staining reveals numerous cells with an undifferentiated, mesenchymal morphology on the right side of the head, which received the graft. (A) Mesenchymal cells on the left side, which did not receive the graft, do not show presence of the fluorescein dextran label. Level of cross-section in A and B corresponds approximately with the line depicted in Fig. 2G. Notes: in both images, dorsal is up, ventral is down; scale bar, 25  $\mu$ m.

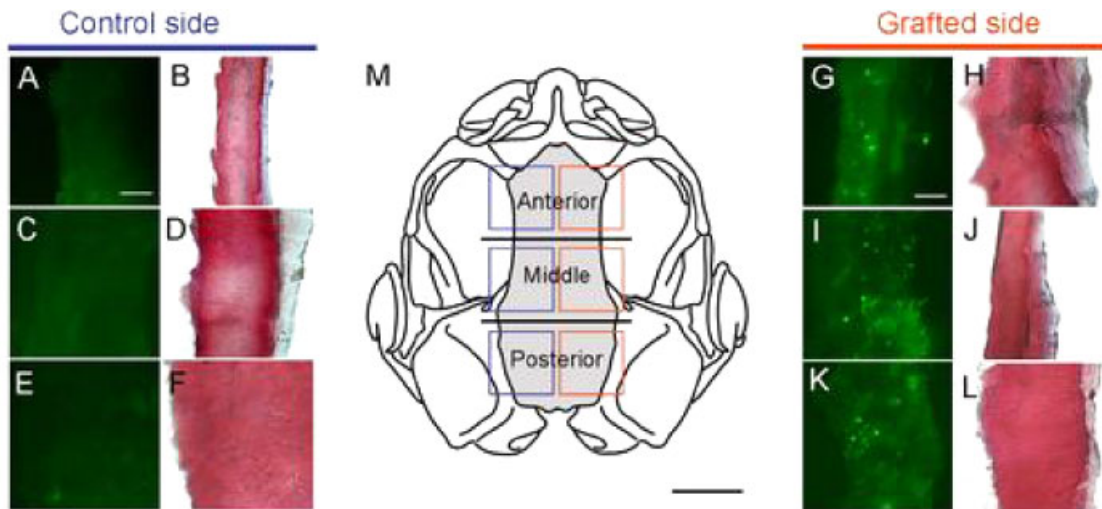


Fig. 4. The CNC contributes, at least in part, to the entire anteroposterior extent of the frontoparietal bone in *X. laevis*. Fluorescent (A, C, E and G, I, K) and bright-field (B, D, F and H, J, L) images of frontal plane cryosections through the anuran frontoparietal in chimeric froglets at stage 66 are shown. Successive portions correspond to squares that are superimposed on a dorsal schematic of an NF stage 66 froglet skull in M (frontoparietal bone is gray). Grafting labeled mandibular CNC yields brightly labeled bone matrix in the anterior frontoparietal (G, green punctate clusters;  $n = 4$ ); presence of labeling of bone matrix is confirmed by TriChrome staining in the following section (H, red). Similarly, middle (I, J;  $n = 4$ ) and posterior (K, L;  $n = 3$ ) portions of the frontoparietal bone matrix are labeled with CNC cells derived from hyoid and branchial stream grafts, respectively. Note the absence of the marker on the control (left) side of the skull, which did not receive labeled CNC grafts (A–F). Black horizontal lines in M demarcate the equal sized zones corresponding to the “anterior,” “middle,” and “posterior” regions analyzed in the frontoparietal. Scale bars: A–L, 25  $\mu$ m; M, 1 mm.

23°C) overnight. Embryos were assessed for survival and brightness of fluorescence prior to grafting such that only the healthiest, most brightly fluorescing embryos were selected for subsequent experiments.

### ***Embryonic grafting***

Embryo grafting was carried out at Nieuwkoop and Faber (NF) stage 14. Tissue explants of small portions of the cranial neural crest (specifically, cells within the neural folds beneath overlying neuroepithelium) that correspond to either the mandibular, hyoid or branchial premigratory streams were grafted from labeled donor embryos into unlabeled hosts following standard procedures (Fig. 1; Sadaghiani and Thiébaud, '87; Zernicka-Goetz et al., '96; Borchers et al., 2000; Carl et al., 2000; Gross and Hanken, 2004). All grafting was carried out unilaterally, on the right side. Thus, the left side of the developing head served as an internal negative control. Analysis of each migratory stream was performed on separate embryos grouped either as mandibular stream-labeled chimeras, hyoid stream-labeled chimeras, or branchial stream-labeled chimeras.

In each case, a portion of the CNC (e.g., mandibular graft) was first removed from an unlabeled host embryo and replaced with an equivalent-sized graft of the same region of the CNC from a labeled, donor embryo. Because cells of the cranial neural crest have the ability to regenerate to some degree following ablation, this methodology was employed to minimize regeneration of the host CNC following grafts. In total, 153 transplants were performed, of which 21 survived through metamorphosis (NF stage 66).

To assess the potential for negative effects of fluorescent dextran on skull development, whole-injected embryos were grown through stage 66, prepared as cleared-and-stained whole mounts, and analyzed for defects (Trueb and Hanken, '92). All control-injected individuals grew normally compared with un-injected siblings; no skeletal defects were observed (data not shown).

### ***Histological analysis***

In *X. laevis*, the frontoparietal bone develops from laterally paired centers of ossification, which later grow toward the midline and fuse to form a single bone in the adult. The frontoparietal is the first bone to differentiate in the tadpole skull, around stage 54, and is fully visible by stage 66 (Trueb and Hanken, '92).

Chimeric embryos were reared to either NF stage 41 or stage 66 and assessed for the presence of the CNC lineage marker (fluorescein dextran) in whole-mount or serial sections, by using a rabbit polyclonal antibody directed against fluorescein tagged to the injected dextran. Stage 41 tadpoles were analyzed in whole-mount (Fig. 2) to determine the regional distribution of labeled CNC cells in the cranial region. They were also analyzed in cryosections (Fig. 3) to determine the distribution of labeled CNC cells and extent to which cranial mesenchyme is derived from the neural crest. Stage 66 specimens were analyzed only in cryosections (Fig. 4) cut in the frontal plane directly through the frontoparietal bone to ensure that positively identified fluorescent dextran label was present within the bone matrix, rather than on the surface.

All animals were fixed overnight in 3.7% PFA at 4°C. Following fixation, specimens were rinsed several times in PBS and the heads removed from the body for immunohistological processing. For whole-mount staining, tissues first were blocked in a solution of 5% normal goat serum in PBT (PBS + 0.1% Triton X-100) for 2 hr at room temperature. The exogenously applied fluorescein dextran was detected immunohistochemically using a rabbit anti-fluorescein polyclonal antibody (1:250 dilution; catalog number A-889; Molecular Probes, Eugene, OR) overnight at 4°C. The next morning, tissues were rinsed in PBS and then incubated overnight in goat anti-rabbit Alexa 488 secondary antibody (1:500 dilution; catalog number A-11008; Molecular Probes). The following morning, specimens were rinsed and mounted in Fluoromount G (Southern Biotech, Birmingham, AL) prior to viewing with fluorescent illumination.

For sectioned tissue analysis, heads were sunk and embedded in Tissue Tek OCT compound (Electron Microscopy Sciences, Hatfield, PA), sectioned at 16- $\mu$ m thickness, and collected on to Superfrost Plus glass slides (VWR Scientific, West Chester, PA) for immunohistochemical processing (same immunohistochemical method as above). Stage 66 skull bone sections were processed in several ways: (1) chromatic staining of cartilage and bone, (2) immunofluorescent staining for the presence of the neural crest cell label (methods above), or (3) immunofluorescent staining but with no primary antibody (as a negative control). Sections showing positive staining for the injected dextran label were verified against negative controls (data not shown). Positive dextran staining in bone was verified by comparing the stained

region with sections on the next sequential slide, which was stained for bone (Direct Red) using a standard TriChrome histological staining protocol (Presnell and Schreiber, '97). The entire frontoparietal bone was divided into three approximately equal sized zones corresponding to "anterior," "middle," and "posterior" regions (Fig. 4).

### Image acquisition

Specimens were mounted using Fluoromount G (Southern Biotech) and viewed with a Leica fluoroscope (Model DMRE; sectioned specimens) or a Leica dissecting fluoroscope (Model MZFLIII; whole mounts). High-resolution digital images were obtained with a 12-bit, black-and-white CCD camera (ORCA, Hamamatsu, Bridgewater, NJ) using Openlab software (Improvision, Coventry, United Kingdom). Images were saved as TIFF files, pseudocolored, and contrast-adjusted in Adobe Photoshop 7.0 for Macintosh.

## RESULTS

All three embryonic migratory streams of the CNC contribute to the frontoparietal bone in adult *X. laevis*. Using a method of focal grafting of fluorescent dextran-labeled regions of the CNC that are destined to give rise to mandibular, hyoid, and branchial streams, we have established the direct cellular contribution of each migratory stream to the dermal skull roof following metamorphosis (Fig. 4).

Roughly 24 hr following embryonic grafting, cells within the mandibular, hyoid, and branchial streams migrate from the dorsal portion of the head (Fig. 1). These streams remain distinct from one another over the course of tadpole development (Fig. 2). Before bone differentiation, numerous labeled but undifferentiated cells were visible in the most dorsal portion of the head just lateral to the developing brain and beneath the overlying epidermis (Fig. 3). By this point in development, labeled mesenchymal cells were observed rostrally as far as the nares (Fig. 2B), laterally to the side of the head (Fig. 2B, D, and F), and caudally to the

level of the posterior margin of the ceratobranchial cartilages (Fig. 2F). Following metamorphosis, labeled cells from the three streams coalesce to form the frontoparietal bone (Fig. 4). Labeled neural crest-derived cells were observed within the bone along its entire length.

The mandibular (anterior) stream gives rise to the anterior-most portions of the frontoparietal. Conversely, the hyoid (middle) and branchial (posterior) streams contribute to the middle and posterior-most parts of the frontoparietal, respectively (Fig. 4G–L). All grafts were unilateral and performed only on the right side. As expected, there was no indication of a contribution of labeled cells to the left side of the developing skull from any grafted CNC explant (Fig. 4A–F).

Populations of migratory CNC cells retain their initial anteroposterior boundaries during larval development. In the three types of chimeras examined, punctate clusters of labeled mesenchymal cells remain anteriorly distributed in the mandibular (anterior) CNC stream grafts, medially distributed in the hyoid (middle) grafts, and posteriorly distributed in the branchial (posterior) grafts (Fig. 2). Thus, derivatives of the three migratory streams of CNC remain distributed in the head according to their relative embryonic positions within the neural fold, following labeling, during larval development, and after initiation of osteogenesis.

## DISCUSSION

### *Comparative and phylogenetic aspects of CNC contributions to the vertebrate skull vault*

We report a substantial contribution of embryonic CNC to the adult frontoparietal bone in *X. laevis*. The contribution extends along the entire length of the bone and is derived from all three CNC streams. This is the first direct evidence of a CNC origin of the anuran osteocranium, although various researchers have long posited such a role in amphibians (Raven, '31; Andres, '46; Sellman, '46). de Beer, in a study of neural crest contribution to cranial cartilages and teeth in the sala-

TABLE 1. Reports describing the embryonic derivation of the skull vault in the domestic chicken (*Gallus gallus*)<sup>1</sup>

Bones of the skull vault	Le Lièvre ('78)	Noden ('78, '82)	Couly et al. ('93)	Le Douarin and Kalcheim ('99)
Frontal	CNC/MD	CNC/MD	CNC	CNC
Parietal	MD	n/s	CNC	CNC

<sup>1</sup>Abbreviations: CNC, cranial neural crest; MD, mesoderm; n/s, not specified in this report.

mander *Ambystoma*, observed “the only cells present on the site of the future splenial bone [in the lower jaw]...are also ectomesenchyme [of CNC origin] from which it must be surmised that the bone will arise” (’47: p 386). Subsequently, Wagner (’49) reported neural crest derivation of the premaxilla, dentary, splenial, and vomeropalatine bones in newts (*Triturus*) based on analysis of salamander–frog chimeras. None of these studies succeeded in labeling embryonic neural crest and subsequently resolving the label in the bony skull following metamorphosis.

Our experimental protocol does not enable us to assess the possible contribution of cranial mesoderm to the frontoparietal, as has been reported in amniotes (reviewed in Santagati and Rijli, 2003). Therefore, we cannot evaluate whether CNC is the sole source of osteogenic cells of the frontoparietal bone in *Xenopus* or, instead, if CNC and mesoderm both contribute cells. It is significant, however, that CNC contributes to the entire length of the frontoparietal in *Xenopus*. This pattern of derivation is identical to that reported for the domestic chicken (Couly et al., ’93). This pattern is different from studies reported for the mouse, in which CNC contribution to the skull vault is limited to the frontal, while the parietal forms solely from mesoderm (Morriss-Kay, 2001; Jiang et al., 2002; Ishii et al., 2003; Jeong et al., 2004).

Comparison with these vertebrates, and evolutionary inferences regarding cranial evolution based on such comparison, are complicated by conflicting accounts regarding the extent of neural crest contribution in birds. Embryonic fate maps for the chicken derived from analysis of quail–chick chimeras offer different patterns of CNC contribution to the skull vault (Table 1). Early reports claimed that only the most anterior part of the frontal bone was derived from CNC (Le Lièvre, ’78; Noden, ’78, ’82). Later reports extended the CNC-derived territory caudally to include not only the entire frontal bone, but also the more posterior parietal bone (Couly et al., ’93; Le Douarin and Kalcheim, ’99). Discrepancies between early and late accounts have been attributed to differences in experimental protocols that involve the timing of embryonic grafting and the stage at which chimeras were later analyzed (Couly et al., ’93; Morriss-Kay, 2001). This interpretation remains to be validated by additional experimental analysis.

The most parsimonious explanation of a shared pattern of neural crest derivation of frontal and parietal bones in amphibians and birds is that this pattern represents the plesiomorphic (primitive)

condition of skull vault development in tetrapods from which alternate patterns, such as that in the mouse, evolved. Alternatively, similar patterns in amphibians and birds may have evolved independently from a different pattern found in their common ancestor, which may or may not have resembled that seen in the mouse.

Finally, amphibians, birds, and mammals may ultimately be shown to possess unique patterns of neural crest derivation of the skull vault that are not shared between any two of these taxa. Existing data do not allow us to decide among these alternate evolutionary scenarios. However, demonstration of apparent differences among at least some major groups of tetrapods suggests that the pattern of neural crest derivation of the skull is evolutionarily labile and has not been rigidly conserved during vertebrate history.

Comparative analysis of patterns of neural crest contribution to the skull vault among major tetrapod clades relies critically on current interpretations of the homology of the bones involved; it assumes that the anuran frontoparietal is the “same” bone as the frontal and parietal of birds and mammals, etc. Indeed, different patterns of neural crest contribution to these bones among classes could be regarded as evidence that the neural crest–mesoderm boundary has shifted during vertebrate evolution. An alternate interpretation is that the neural crest–mesoderm interface is evolutionarily invariant and that our current understanding of bone homologies for the skull vault among tetrapods is incorrect. Many of these homologies were defined during an earlier period of comparative morphology (e.g., Parker and Bettany, 1877; de Beer, ’47) that predates application of rigorous methods for phylogenetic reconstruction and character analysis (e.g., Harvey and Pagel, ’91) as well as numerous recent discoveries and analyses that have yielded a much more robust understanding of tetrapod origins and relationships (Ruta et al., 2003). In light of the abundant new data regarding both cranial development and phylogeny of vertebrates, re-assessment of homologies of the skull vault is warranted. We especially urge evaluation of the hypothesis that frontal and parietal bones, as currently defined, may not be homologous across all major groups of extant tetrapods.

### *Developmental questions*

Neural crest derivation of the bony skull in *Xenopus* begs the question of where cranial

osteogenic precursor cells reside between embryogenesis, when they emerge from the neural folds as CNC, and metamorphosis, when they differentiate into osteocytes. We observed many labeled mesenchyme cells in the dorsal portion of the head during larval development. Because there exists no known marker for undifferentiated osteogenic cells, it is not possible to determine if these neural crest-derived cells are committed to form bone or if they will ultimately contribute to the skull. However, given their location, we regard them as prime candidates for cranial bone precursors.

In *X. laevis*, all three CNC streams contribute to the frontoparietal bone. Such a composite CNC participation in bone formation has already been reported in birds, in which both mandibular and hyoid stream neural crest cells join to form the jaw skeleton (Köntges and Lumsden, '96). Cell populations within the proximal articular bone that are derived from different neural crest streams are adjacent to one another and largely overlapping. Moreover, boundaries between these different cell populations do not coincide with any obvious anatomical boundaries within the bone. In *Xenopus*, each cranial neural crest stream also appears to populate a different region of the frontoparietal bone, and boundaries between adjacent regions do not coincide with any visible osteological boundaries or comparable landmarks.

### ***Fluorescent dextrans as long-term cell markers***

In this study, fluorescent dextran has been employed as a stable and reliable molecular cell marker that persists through the protracted larval period that precedes bony skull formation in metamorphosing frogs (Gross and Hanken, 2004). We encourage incorporation of this labeling technique in comparable studies of the embryonic origin of adult features of other organisms, but especially to nonmodel species that currently are beyond the reach of sophisticated genetic procedures, such as transgenesis. When conducted within an appropriate phylogenetic context, results likely will increase our understanding of the developmental mechanisms that underlie morphological differences between disparate taxonomic groups.

### **ACKNOWLEDGMENTS**

We thank members of the Hanken laboratory for critical comments on the manuscript. Drew Noden generously provided an English summary

of Wagner ('49). Research support was provided by the U.S. National Science Foundation (EF-0334846), the Milton Fund of Harvard University, and Sigma Xi.

### **LITERATURE CITED**

- Andres G. 1946. Über Induktion und Entwicklung von Kopforgangen aus Unkenektoderm in Molch (Epidermis, Plakoden und Derivate der Neuralleiste). *Rev Suisse Zool* 53:502–510.
- Borchers A, Epperlein HH, Wedlich D. 2000. An assay system to study migratory behavior of cranial neural crest cells in *Xenopus*. *Dev Genes Evol* 210:217–222.
- Carl TF, Vourgourakis Y, Klymkowsky MK, Hanken J. 2000. Green fluorescent protein used to assess cranial neural crest derivatives in the frog, *Xenopus laevis*. In: Jacobson C-O, Olsson L, editors. *Regulatory processes in development*. London: Portland Press. p 194.
- Chibon P. 1967. Nuclear labeling by tritiated thymidine of neural crest derivatives in the amphibian *Pleurodeles waltlii*. *J Embryol Exp Morphol* 18:343–358.
- Couly GF, Coltey PM, Le Douarin NM. 1993. The triple origin of the skull in higher vertebrates: a study in quail-chick chimeras. *Development* 117:409–429.
- de Beer GR. 1937. *The development of the vertebrate skull*. Oxford: Clarendon Press. 552 p.
- de Beer GR. 1947. The differentiation of neural crest cells into visceral cartilages and odontoblasts in *Amblystoma*, and a re-examination of the germ-layer theory. *Proc R Soc Lond B Biol Sci* 134:377–398.
- Gross JB, Hanken J. 2004. Use of fluorescent dextran conjugates as a long-term marker of the osteogenic neural crest in frogs. *Dev Dynam* 230:100–106.
- Harvey PH, Pagel MD. 1991. *The comparative method in evolutionary biology*. Oxford: Oxford University Press.
- Hörstadius S. 1950. *The neural crest: its properties and derivatives in the light of experimental research*. London: Oxford University Press. 111 p.
- Ishii M, Merrill AE, Chan YS, Gitelman I, Rice DP, Sucov HM, Maxson RE Jr. 2003. *Msx2* and *Twist* cooperatively control the development of the neural crest-derived skeletogenic mesenchyme of the murine skull vault. *Development* 130:6131–6142.
- Jeong J, Mao J, Tenzen T, Kottmann AH, McMahon AP. 2004. Hedgehog signaling in the neural crest cells regulates the patterning and growth of facial primordia. *Genes Dev* 18:937–951.
- Jiang X, Iseki S, Maxson RE, Sucov HM, Morriss-Kay GM. 2002. Tissue origins and interactions in the mammalian skull vault. *Dev Biol* 241:106–116.
- Köntges G, Lumsden A. 1996. Rhombencephalic neural crest segmentation is preserved throughout craniofacial ontogeny. *Development* 122:3229–3242.
- Landacre FL. 1921. The fate of the neural crest in the head of Urodeles. *J Comp Neurol* 33:1–43.
- Le Douarin NM, Kalcheim C. 1999. *The neural crest*. Cambridge: Cambridge University Press. 445 p.
- Le Lièvre CS. 1978. Participation of neural crest-derived cells in the genesis of the skull in birds. *J Embryol Exp Morphol* 47:17–37.
- Morriss-Kay GM. 2001. Derivation of the mammalian skull vault. *J Anat* 199:143–151.

- Nieuwkoop PD, Faber J, Kirschner MW. 1994. Normal table of *Xenopus laevis* (Daudin). New York: Garland Publishing Inc. 252 p.
- Noden DM. 1978. The control of avian cephalic neural crest cytodifferentiation. I. Skeletal and connective tissues. *Dev Biol* 67:296–312.
- Noden DM. 1982. Patterns and organization of craniofacial skeletogenic and myogenic mesenchyme: a perspective. In: Sarnat BG, editor. *Progress in clinical and biological research: factors and mechanisms influencing bone growth*. New York: Alan R. Liss, Inc. p 657.
- Parker WK, Bettany GT. 1877. *The morphology of the skull*. London: Macmillan. 368 p.
- Presnell J, Schreibman M. 1997. *Humason's animal tissue techniques*. Baltimore: The Johns Hopkins University Press. 572 p.
- Raven CP. 1931. Zur Entwicklung der Ganglienleiste. I: Die Kinematik der Ganglienleistenentwicklung bei den Urodelen. *Roux Arch Entwicklungsmech Org* 125:210–292.
- Ruta M, Coates MI, Quicke DLJ. 2003. Early tetrapod relationships revisited. *Biol Rev* 78:251–345.
- Sadaghiani B, Thiébaud CH. 1987. Neural crest development in the *Xenopus laevis* embryo, studied by interspecific transplantation and scanning electron microscopy. *Dev Biol* 124:91–110.
- Santagati F, Rijli FM. 2003. Cranial neural crest and the building of the vertebrate head. *Nat Rev Neurosci* 4:806–818.
- Sellman S. 1946. Some experiments on the determination of the larval tooth in *Amblystoma mexicanum*. *Odontol Tidsk* 54:1–1238.
- Sive HL, Grainger RM, Harland RM. 2000. *Early development of Xenopus laevis*. Plainview, NY: Cold Spring Harbor Laboratory Press. 338 p.
- Stone L. 1926. Further experiments on the extirpation and transplantation of mesectoderm in *Amblystoma punctatum*. *J Exp Zool* 44:95–131.
- Trueb L. 1985. A summary of the osteocranial development in anurans with notes on the sequence of cranial ossification in *Rhinophrynus dorsalis* (Anura: Pipidae: Rhinophrynidae). *South Afr J Sci* 81:181–185.
- Trueb L, Hanken J. 1992. Skeletal development in *Xenopus laevis* (Anura: Pipidae). *J Morphol* 214:1–41.
- Wagner G. 1949. Die Bedeutung der Neuralleiste für die Kopfgestaltung der Amphibienlarven: Untersuchungen an Chimären von *Triton* und *Bombinator*. *Rev Suisse Zool* 56:519–620.
- Zernicka-Goetz M, Pines J, Ryan K, Siemering KR, Haseloff J, Evans MJ, Gurdon JB. 1996. An indelible lineage marker for *Xenopus* using a mutated green fluorescent protein. *Development* 122:3719–3724.